

On the Mechanism of Soot Track Formation: Numerical Study

Kazuaki INABA* and Akiko MATSUO**

Department of Mechanical Engineering, Keio University, 3-14-1 Hiyoshi, Kohoku-ku, Yokohama 223-8522, JAPAN

* Graduate Student, e-mail: harlock_kazz@1999.jukuin.keio.ac.jp, **Assistant Professor

Katsumi TANAKA

National Institute of Advanced Industrial Science and Technology, Tsukuba 305-8565, JAPAN

Amy K.W. LAM[†], Florian PINTGEN[†], Eric WINTENBERGER[†], Joanna AUSTIN[†], and Joseph E. SHEPHERD[‡]

Graduate Aeronautical Laboratories, California Institute of Technology, Pasadena, CA 91125, USA

[†]Graduate Student, [‡]Professor

Key Words: Soot track, Detonation, Cellular structure, Mach reflection, Boundary layer

1. Introduction

For over 40 years¹, the soot track method has been widely applied as an indication of detonation propagation and a semi-quantitative tool for measuring the cell size and classifying the regularity of the cellular structure. It is readily apparent and demonstrated experimentally² that the soot tracks are associated with the transverse waves and triple points that move along the main shock front. Numerical simulations of detonation have variously used peak pressure, vorticity, and reaction intensity as soot track surrogates, and contours of these quantities produce reasonable facsimiles of soot tracks. However, the precise physical mechanism that creates the soot tracks has never been clearly demonstrated and it is not known what feature of the triple point structure the soot tracks represent. Speculation on the mechanism has included "scrubbing" the soot off by vortices, pushing the soot with pressure gradients, and combustion of the soot in hot oxidizing atmospheres.

The goal of the present study is to explore an alternative explanation that is based on the classical fluid mechanics of near-wall flow in a viscous gas. We propose that the soot tracks are due to variations in the direction and magnitude of the shear stress created by the boundary layer adjacent to the soot foil. Our proposal is motivated by three key observations: 1) soot tracks can be formed in Mach reflection of a non-reactive shock³, 2) pattern formation in oil flow visualization can be completely explained in terms of surface shear stress variations, and 3) the process of Mach reflection in a non-reactive gas contains all the essential features of the transverse wave-main shock interactions in detonation fronts. We examine this hypothesis through numerical simulation of Mach reflection and the associated boundary layers in order to predict the shear stress that will be produced on a soot foil. A simple model of soot motion is used to interpret the effect of shear stress spatial and temporal variations on soot motion. A companion paper⁴ examines the experimental aspects of this hypothesis.

2. Numerical setup

The flow behind the shock wave was investigated by numerically simulating the three-dimensional compressible Navier-Stokes equations. This simulation includes the laminar boundary layers on the soot foil. The governing equations are integrated explicitly. As a numerical scheme, Yee's non-MUSCL type TVD upwind explicit scheme⁵ is utilized. Initial conditions are listed in Table 1. Here, φ_w is a wedge angle, and Reynolds number Re is detected from the computational domain length along the x direction and Mach number M .

Table 1. Initial conditions and triple point track angles.

case	M	$\alpha_w [^\circ]$	$T_1 [K]$	$Re [1/m]$	Simulations [$^\circ$]	Experiments [$^\circ$]	Three-shock theory [$^\circ$]
A	1.9	15	298.15	7.92E6	16	16	17
B	1.2	15	298.15	5.00E6	11	8-9	*11
C	1.9	25	298.15	7.92E6	11	9	11
D	1.2	25	298.15	5.00E6	6	4-5	-

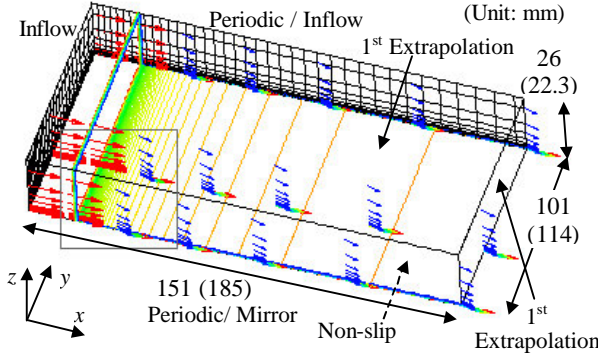
*The glancing incidence theory⁷.

Fig. 1. Boundary conditions and Initial conditions.

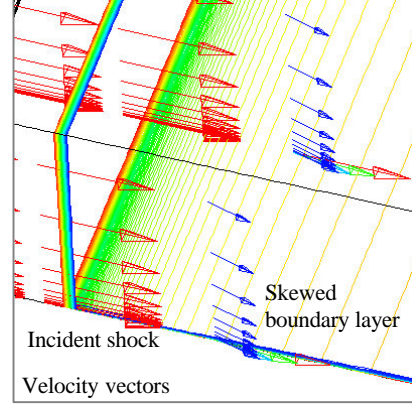


Fig. 2. Enlargement of Fig. 1.

As shown in Fig. 1, a stretched grid system is used and the number of grid points is 151x101x26. The computational domain is 185 mm by 114 mm by 22.3 mm. We adopt a shock-fixed coordinate system; the bottom x-y plane (a non-slip and isothermal boundary condition) corresponds to a soot foil and is moving at the same speed as the shock⁶. Initial conditions are calculated in which the incident shock and a developed, skewed boundary layer exist (Fig. 2). The skewed boundary layer appears to be due to the difference in the direction between the wall and the flow behind the incident shock. Computations for a Mach reflection are started by sudden conversion of sidewall conditions from periodic boundaries to mirror and inflow boundaries. The other boundary conditions are obtained from the first order extrapolations.

3. Results and Discussion

3.1 Flow features

Triple point track angles obtained in numerical simulations are presented in Table 1 with experimental and theoretical⁷ results. The triple point track angles in numerical simulations agree well with the experimental and analytical triple point track angles. The flow features of the wedge angle 25° case do not differ essentially from those of the 15° case, and, therefore, we will discuss only the results of the wedge angle 15° case.

Figure 3 shows the density contour distributions of case A. In a simulation, the triple point moves upward in the y direction because the triple point is not stationary in this frame. Figure 3a shows the bottom flow profile ($z=0.0$) close to the wall and 3b shows the upper flow profile ($z=0.12$). In Fig. 3b, a shear layer SL extending from the triple point is clearer than that in Fig. 3a. Figure 3b indicates the typical flow feature of Single Mach Reflection (SMR)^{8,9}. Three-dimensional boundary layer effects obscure the well-defined shear layer seen in Fig 3a.

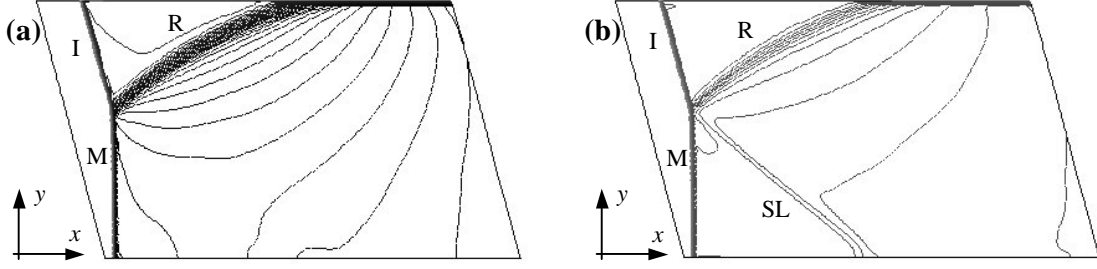


Fig. 3. Density contour distributions of case A: (a) $z=0.0$, near the soot foil, (b) $z=0.12$, upper boundary (I: Incident shock, M: Mach stem, R: Reflected shock, SL: Shear Layer).

3.2 Shear stress distributions on the surface

Figure 4 shows a simple model of velocity profiles in gas boundary layer and soot film and with a constant shear stress in the soot layer. If we approximate the soot as an incompressible fluid, the soot thickness \bar{a} obeys the following conservation equation:

$$\frac{\partial \bar{d}}{\partial t} + \nabla_{x,y} \cdot (\bar{d} \cdot \bar{u}_{soot}) = 0 \quad (1), \quad \bar{u}_{soot} = \frac{\bar{d} \cdot \bar{\tau}_{gas}}{2m_{soot}} \quad (2)$$

Hence, the key for understanding the soot thickness redistribution by the shock front is to obtain the distribution of shear stress $\bar{\tau}_{gas}$.

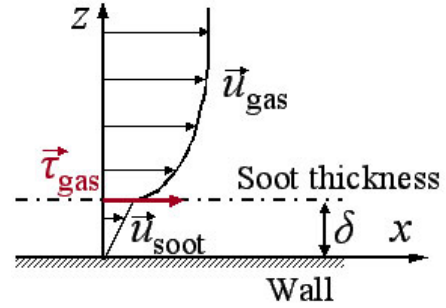


Fig. 4. Schematic diagram of shear stress effect on soot.

Instantaneous shear stresses in the gas at the bottom x-y plane of the computational domain are derived from the simulation results. In the shock stationary frame, the wall shear stress is opposite in sign to that in the lab frame. Figure 5a displays the magnitude contours and the vectors of shear stress magnitude $|\partial|$ in case A. Shear stresses ∂_{xz} decrease as a function of a distance from the shock. For an ideal shock wave (zero thickness), the peak shear stress at the shock will be infinite. Due to the finite thickness of the shock wave in the numerical simulation, the shear stress is finite at the front and the magnitude of the peak is dependent on the mesh size. Although the difference in the shear stress just behind the incident shock ($y=0.42$) and the Mach stem ($y=0.30$) is just about 25%, the shear stress ∂_{yz} (in Fig. 5b) indicates a remarkable difference behind the two shocks. The shear stress ∂_{yz} just behind the incident shock ($y=0.42$) equals 25% of the shear stress ∂_{xz} while shear stress ∂_{yz} between the Mach stem and the shear layer ($y=0.30$) is very small. In Mach reflection experiments⁴, darker soot belts between triple point tracks and wedges are observed. It is reasonable to suppose that these darker belts are formed by the effect of the variation of the shear stress ∂_{yz} . According to Fig. 5, shear stresses behind the incident shock and Mach stem intersect at the triple point track, and this effect will act to pile up soot, forming a track. Further analyses on the soot thickness \bar{a} are in progress on this aspect of the problem.

4 Summary

Mach reflections over a wedge were successfully performed in three-dimensional numerical simulations. The soot

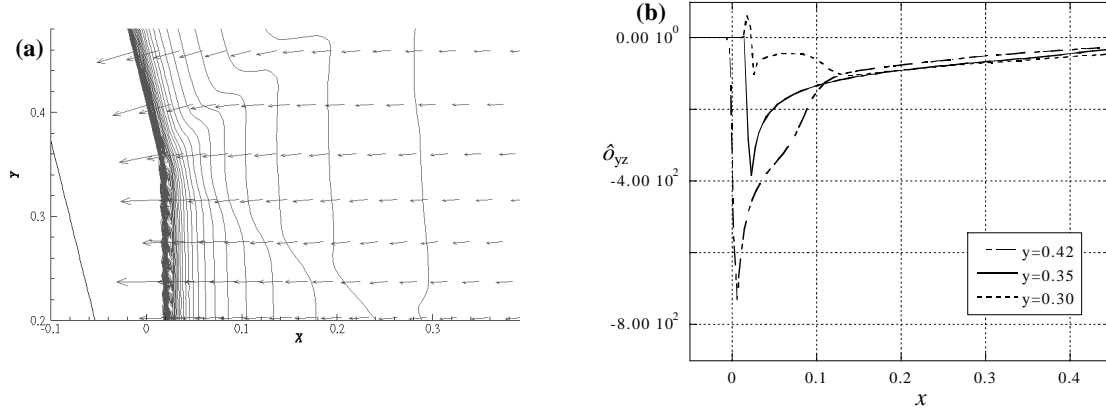


Fig. 5. Shear stress in case A, (a) contours and vectors of magnitude $|\delta|$, (b) δ_{yz} profile along x axis.

track angles obtained in numerical simulations were consistent with the experimental and theoretical triple point track angles. We concluded from our simulation results that the soot gathered along the shear layer due to the variation of the component of shear stress parallel to the front and formed the darker soot belt inside the Mach stem funnel.

Acknowledgments

This work was supported by the Research Fellowships of the Japan Society for the Promotion of Science for Young Scientists. The authors acknowledge several discussions with Prof. H. Hornung.

Reference

- ¹ Yu. N. Denisov and Ya. K. Troshin, *Dokl. Akad. Nauk SSSR (Phys-Chem. Sect.)* 125, (1959), pp.110-113.
- ² J. H. Lee, R. I. Soloukhin, and A. K. Oppenheim, *Astronaut. Acta*, 14, (1969), pp.565-584.
- ³ E. Mach and J. Wosyka, *Sitzungsber Akad Wiss Wien (II.Ab)*, 72, (1875), pp. 44-52.
- ⁴ A. K. W. Lam, K. Inaba, F. Pintgen, E. Wintenberger, J. Austin, A. Matsuo, and J. E. Shepherd, in *Proc. 19th ICDERS*, Japan.
- ⁵ H. C. Yee, NASA TM 89464, (1987).
- ⁶ B. Sturtevant and T. T. Okamura, *Phys. Fluids*, 12, (1969), pp. 1723-1725.
- ⁷ Ames Research Staff, "Equations, tables and charts for compressible flow," NACA Rep. 1135, (1953).
- ⁸ G. Ben-Dor, "Shock wave reflection phenomena", Springer- Verlag, New York, (1991).
- ⁹ H. Hornung, *Ann Rev. Fluid Mech.*, 18, (1996), pp. 33-58.